Recurrent *EZH1* mutations in autonomous thyroid adenomas (Calebiro *et al.*)

Supplemental data

Supplemental Methods

Tissue samples, patients and clinical annotations

Patients were recruited at the following participating institutions: Division of Endocrinology and Nephrology, University of Leipzig, Leipzig, Germany; Division of Endocrine and Metabolic Diseases, IRCCS Istituto Auxologico Italiano, Milan, Italy; Department of Pediatric Endocrinology and Rheumatology, Poznan University of Medical Sciences, Poznan, Poland; Division of Endocrinology and Metabolism, Marmara University Medical School, Istanbul, Turkey. Clinical data and patient samples were then centralized at the following two referral centers: Division of Endocrinology and Nephrology, University of Leipzig, Leipzig, Germany; Division of Endocrine and Metabolic Diseases, IRCCS Istituto Auxologico Italiano, Milan, Italy. The diagnosis of ATA was based on clinical and biochemical data and was confirmed by histological examination. The clinical data, methods and results of the previous *TSHR* and *GNAS* mutation screening of the samples from Germany and Turkey have been reported previously (1-3).

We collected 19 fresh frozen ATA samples with corresponding normal thyroid tissues for next generation whole-exome sequencing. Of these, five ATAs were subsequently found to carry activating *TSHR* mutations, which were not detected by conventional screening methods. Clinical parameters, such as sex, age at surgery, tumor size, and results of hormone tests are shown in **Supplemental Table 4**.

In addition we analyzed an independent set of thyroid samples (n=304): 94 ATAs diagnosed in adults and characterized previously for the occurrence of *TSHR* mutations (n=59 (2); n=35 (1)), 29 ATAs diagnosed in children and adolescents (< 19 years; Ref. 3), 59 normal surrounding tissues of ATAs (NSTs), 82 CTNs, 16 FTCs, and 24 PTCs. Of the 94 adult ATA samples, 64 were from solitary ATAs and 30 were from toxic

multinodular goiters. The lack of correlation of available clinical parameters with the absence/presence of *TSHR* mutations and the *in vitro* activity of the respective *TSHR* mutations in ATAs have been previously reported (4, 5).

DNA was extracted using the QIAamp DNA Mini Kit (Qiagen) according to the manufacturer's recommendations.

Whole-exome sequencing and data analysis

Exomes were enriched in solution and indexed with the use of the SureSelect XT Human All Exon 50Mb kit, version 5 (Agilent Technologies). Sequencing was performed as paired-end reads of 100 bp on HiSeq2500 systems (Illumina).

Pools of 12 indexed libraries were sequenced on four lanes to an average depth of coverage between 100x and 140x. Image analysis and base calling was performed using Illumina Real Time Analysis. Reads were aligned against the human assembly hg19 (GRCh37) using Burrows-Wheeler Aligner (BWA v 0.7.5a). We performed single-nucleotide variant and small insertion and deletion (indel) calling specifically for the regions targeted by the exome enrichment kit, using SAMtools (v 0.1.18) and custom scripts. Subsequently, the variant quality was determined using the SAMtools varFilter script. We used default parameters, with the exception of the maximum read depth (-D) and the minimum P-value for base quality bias (-2), which we set to 9999 and 1e-400, respectively. Additionally, we applied a custom script to mark all variants with adjacent bases of low median base quality. All variants were then annotated using custom Perl scripts. Annotation included information about known transcripts (UCSC Known Genes and RefSeq genes), known variants (dbSNP v 135), type of mutation and – if applicable – amino acid change in the corresponding protein. The annotated variants were then inserted into our in-house database. To discover putative somatic variants, we queried our database to show only those variants of a tumor that were not found in the corresponding control tissue. To reduce false positives we filtered out variants that were already present in our database, had a variant quality of less than 40, or failed one of the filters from the filter scripts.

We then manually investigated the raw read data of the remaining variants using the Integrative Genomics Viewer (IGV). The possible functional impact of the newly identified variants was investigated using the PolyPhen-2 (Polymorphism Phenotyping v2) software, a tool that predicts the possible impact of an amino acid substitution on the structure and function of a human protein using physical and homology information (6). The c.1712A>G substitution was not present in 6,951 in-house exomes nor in 60,706 exomes of the Exome Aggregation Consortium (ExAC) browser version 0.3 (7). The Gene Ontology enRIchment anaLysis and visuaLizAtion tool (Gorilla) was used to identify enriched gene ontology (GO) terms (8). The Gene Set Enrichment Analysis (GSEA) software was used to perform canonical pathway analysis (9). Full exome sequencing data is available upon request.

Detection of TSHR and EZH1 point mutations by PCRs using high resolution melting (HRM) analysis

EZH1 and *TSHR* (exons 9 and 10, those exons in which all previous activating *TSHR* mutations were detected) point mutations were detected by real time PCR and HRM, using primers flanking the mutation hotspots (including one biotin-labeled primer for subsequent pyrosequencing) and the LightCycler 480 High Resolution Melting Master chemistry (Roche) on a LightCycler 480 (Roche). PCRs to detect *EZH1* point mutations were processed through an initial denaturation at 95°C for 10 min followed by 55 cycles of a 3-step PCR, including 3 s of denaturation at 95°C, a 10 s annealing phase at 60°C, and an elongation phase at 72°C for 10 s. PCRs to detect *TSHR* point mutations were processed through an initial denaturation at 95°C for 10 min followed by 55 cycles of a 3-step PCR, including 3 s of denaturation at 95°C, a 10 s annealing phase at 56°C, and an elongation phase at 72°C for 10 s. as recently published (3). Thereafter, a high resolution melting curve was assessed from 75°C to 95°C with an increase of 0.02°C/s and 25 acquisitions per degree.

Samples tested suspicious for *EZH1* mutations were subsequently analyzed by pyrosequencing on a PyroMark Q24 (Qiagen, Hilden, Germany). Samples tested suspicious for *TSHR* mutations were subsequently analyzed by pyrosequencing on a PyroMark Q24 or were sequenced using Big Dye-terminator

chemistry (Applied Biosystems) according to the manufacturer's instructions and analyzed on an automatic sequencer (ABI 3100, Applied Biosystems).

Detection of point mutations by pyrosequencing

EZH1 (c.1712A>G) and *TSHR* point mutations (in position c.453, c.623, c.629, c.631, and c.632) were detected by pyrosequencing using self-designed template specific sequencing primers and the PCR products from the HRM-PCRs described above. In brief, 5µl PCR products were immobilized to streptavidin sepharose beads and single stranded DNA was prepared allowing subsequent annealing of the sequencing primer to the template DNA. Then, the primed single stranded DNA was released from the streptavidin surface and transferred to a PyroMark Q24 (QIAGEN) for pyrosequencing.

DNA constructs and site-directed mutagenesis

A plasmid coding for FLAG-tagged wild-type human EZH1 was purchased from Origene. The c.1712A>G mutation was introduced by PCR and the wild-type or mutant EZH1 sequences were subcloned into the pcDNA3 expression vector. Both constructs were verified by direct sequencing.

In silico analysis of EZH1 mutations

Sequence alignments were performed using the CLC Sequence Viewer software (CLC Bio). Structural images were generated using the structure of the catalytic (SET) domain of the highly homologous human EZH2 as template (Protein Data Bank entry 4MI5). The position of the substrate and SAH are based on an alignment with human H3K9 methyltransferase (Protein Data Bank entry 3HNA). The structure of the PRC2 complex is based on the available electron density map (10) and structures of homologous domains from the following Protein Data Bank entries: 3HM5 (SANT), 2QXV (EED), 2YB8 (RbAp48). Structural images were generated using the UCSF Chimera 1.10.2 software (11).

Cell culture and transfection

HEK293-AD cells were purchased from American Type Culture Collection (ATCC). FRT cells were kindly provided by Dr. L. Nitsch (Department of Molecular Medicine and Medical Biotechnology, University of Naples Federico II, 80131 Naples, Italy). PCCL3 cells were a gift from D. Altschuler (Department of Pharmacology and Chemical Biology, School of Medicine, University of Pittsburgh, Pittsburgh, PA 15261, USA). HEK293 and FRT cells were cultured and transfected as previously described (12, 13). FRT cells retain several characteristics of thyroid cells but do not express endogenous TSHR (14). Stable FRT clones expressing the wild-type TSHR receptor or an activating TSHR mutant (V597F) were obtained as previously described (12). TSHR expression was then verified by real-time quantitative PCR and western blot experiments.

For the generation of FRT pools stably expressing either wild-type or Gln571Arg EZH1, FRT cells were transfected with Fugene HD (Promega) with a transfection reagent:DNA ratio of 3:1, following the manufacturer's instructions. The optimal concentration of G418 was determined through concentration-response curves as the 99% growth inhibitory concentration. Three days after the transfection, the cells were put in selection medium containing 500 µg/ml G418 and subsequently expanded. The stable pools were used without subsequent cloning to avoid the effects of clonal variability.

PCCL3 cells were maintained in F-12 Ham Nutrient Mixture (Sigma-Aldrich) supplemented with 5% fetal bovine serum, 0. 1mg/ml streptomycin, 100 U/ml penicillin, 2 mM L-glutamine and a combination of four hormones: 1µg/ml insulin, 1 mU/ml TSH, 5 µg/ml apo-transferrin, 1nM hydrocortisone at 37ºC, 5% CO_2. PCCL3 cells were grown in 100-mm Petri culture dishes to a confluency of ca. 60% and were transfected using Lipofectamine 2000 reagent (Invitrogen) according to manufacturer's instructions. The medium was replaced after 48 hours and the cells were lysed 96 hours post transfection.

Both FRT and PCCL3 cell lines were tested for the presence of the Gln571Arg mutation and were found to be wild-type.

Histone acid extraction

Histones were acid extracted from cells and ATA tissues as described by Shechter et al. (15). Briefly, harvested cells or Douncer-homogenized tissue samples were lysed in a hypotonic lysis buffer (150 mM Tris/HCl, 1 mM KCl, 1.5 mM $MgCl_2$ 1 mM DTT, pH 8.0) supplemented with 0.5 µg/ml leupeptin, 2 µg/ml aprotinin, 0.1 mM phenylmethylsulfonyl fluoride (PMSF) and the cOmplete Mini protease inhibitor cocktail (Roche). The lysates were then acid-extracted with H_2SO_4 followed by precipitation with trichloroacetic acid and resuspended in H_20.

Western blot analysis

Western blot analyses were performed as previously described (13). Briefly, lysates were denatured in Laemmli buffer for 3 minutes at 95ºC. Proteins were then separated on SDS polyacrylamide gels followed by transfer onto polyvinylidene difluoride (PVDF) membranes (Merck Millipore). Subsequently, the membranes were blocked for one hour at room temperature in Tris-buffered saline containing 0.1% Tween 20 (TBS-T) and 5% milk and incubated overnight at 4 °C with the indicated primary antibody. This was followed by incubation with horseradish peroxidase (HRP) conjugated secondary antibodies (Dianova, 1:10,000) for one hour at room temperature and chemiluminescence was detected using a HRP substrate (Amersham, GE Healthcare). The following primary antibodies were used: rabbit polyclonal anti-FLAG (Sigma-Aldrich, F7425, 1:4,000), rabbit polyclonal against total (Abcam, ab1791, 1:5,000), mono-methylated (Millipore, 07-448, 1:1,000), di-methylated (Millipore, 07-452, 1:1,000) or tri-methylated (Millipore, 07-449, 1:1,000) histone H3, rabbit polyclonal anti-EED (Abcam, ab4469, 1:10,000), goat polyclonal anti-Suz12 (Santa Cruz Biotechnology, P-15, sc-46264, 1:10,000), rabbit monoclonal anti-AEBP2 (Cell Signaling, D7C6X, 1:10,000), rabbit polyclonal anti-phospho-histone H3 pSer10 (Thermo Fisher Scientific, PA5-17869, 1:1,000), rabbit monoclonal anti-cyclin D1 (Cell Signaling, 92G2, 2978, 1:1,000) and mouse anti-actin (BD Biosciences, Ab-5, 612657, 1:2,000).

Co-immunoprecipitation

Cell lysis and co-immunoprecipitation experiments were carried out as described by Yap *et al.* (16), with minor modifications. Briefly, 96 h post transfection, cells were lysed in cold isotonic lysis buffer containing 150 mM NaCl, 1.5 mM $MgCl_2$, 10 mM Tris-HCl, pH 7.5 supplemented with 0.5% NP-40, 0.5 µg/ml leupeptin, 2 µg/ml aprotinin, 1 mM PMSF and the cOmplete Mini protease inhibitor cocktail (Roche). The resulting cytosolic and nuclear fractions were separated by centrifugation at 20,000 x *g* for 15 min at 4ºC. The nuclear pellet was resuspended in cold nuclear lysis buffer, consisting of 250 mM NaCl, 20 mM $NaPO_4$, pH7.0 supplemented with 30 mM $Na_4O_7P_2$, 5 mM EDTA, 10 mM NaF, 0.1% NP-40, 10% glycerol, 1 mM dithiothreitol (DTT), 0.5 µg/ml leupeptin, 2 µg/ml aprotinin, 1 mM PMSF and the cOmplete Mini protease inhibitor cocktail (Roche), followed by sonication to disrupt the chromatin. Benzonase (Sigma-Aldrich, final concentration 1U/ml) was added and the lysate was incubated on a horizontal shaker for one hour and then one hour without shaking at 4ºC. The lysate was cleared by centrifuging at 20,000 x *g* for 5 min at 4ºC followed by another round of sonication and centrifugation. An aliquot of the lysate was removed and stored as input and the remainder was diluted with binding buffer (150 mM NaCl, 50 mM Tris-HCl, pH 7.5 supplemented with 0.05% NP-40, 1 mM EDTA, 2 µg/ml aprotinin, 2 µg/ml leupeptin, 1 mM PMSF). The lysate was treated with two rounds of pre-clearing by incubation with protein A Sepharose (GE Healthcare) under continuous rotation, each time for one hour at 4ºC. Pre-clearing was followed by incubation with mouse anti-FLAG antibody (Sigma-Aldrich, F3165, 10 µg per sample) pre-bound to protein A Sepharose for two hours under continuous rotation at 4ºC. Samples were washed five times with binding buffer and proteins were eluted from protein A Sepharose by incubation in Laemmli buffer for 3 minutes at 95ºC. The input and the immunoprecipitated fractions were examined by western blot analysis.

Proliferation Assay and measurement of proliferative markers

The effects on proliferation were assessed in stable FRT clones transiently transfected with either wild type or mutant EZH1 as well as in stable FRT pools expressing wild type or mutant EZH1. FRT cells were plated in 96-well plates and cultured in F-12 Ham Nutrient Mixture (Euroclone) supplemented with 5% fetal calf

serum, 1% penicillin, 1% streptomycin, 2 mM L-glutamine and 500 µg/ml G418 in absence of TSH. Cell viability was measured at different time point utilizing the 3-(4,5-dimetylthiazole-2-yl)-2,5-diphenyltetrazolium bromide (MTT) assay (Sigma-Aldrich).

For the analysis of proliferative markers (cyclin D1 and histone H3 phosphorylated at Ser10) cells were lysed with SDS sample buffer (62.5 mM Tris-HCl pH 6.8, 2% SDS) supplemented with cOmplete Mini protease inhibitor cocktail (Roche) and Phosphatase Inhibitor Cocktail 2 (Sigma-Aldrich), immediately heated for 5 min at 95°C and sonicated. Western blot analysis was performed on whole cell lysates.

Appendix 1: Non-Recurrent Mutations in GPCR Genes

In addition to the well-known *TSHR* mutations, exome sequencing of ATAs identified non-recurrent mutations in other GPCR genes (see **Supplemental Table 1 and 2**). These involved the following 4 genes: *GALR2, OR2G2, OR5M3 and TAS1R2*.

GALR2 codes for the galanin receptor 2, which binds the peptide galanin and is coupled to G_q and G_i. The identified change, Ser112Arg, affects a high conserved Ser residue (3.39 according to the Ballesteros-Weinstein numbering system) in the 3rd trans-membrane domain (3TM) of class A GPCRs (**Supplemental Figure 2**). In a high resolution structure of the α_{2A}-adrenergic receptor (15), the corresponding Ser 3.39 residue is involved in the coordination of a Na^+ ion, which functions as an allosteric modulator of ligand binding. Thus, substitution with Arg, a bulkier and positively charged residue, might alter GALR2 signaling.

OR2G2 and *OR5M3* codes for two olfactory receptors (class A). The mutation in *OR2G2* (Cys192Tyr) affects a Cys residue located in the 2nd extracellular loop. The mutation in *OR5M3* (Arg260His) is located in the 3rd extracellular loop.

TAS1R2 codes for the taste receptor type 1, member 2 (sweet taste receptor). The identified mutation (Gly320Val) lies in the large extracellular domain of this class-C receptor, which is involved in ligand binding.

To the best of our knowledge, no relevant information is available regarding the mutated residues in *OR2G2, OR5M3* and *TAS1R2*.

Supplemental Table 1. Overview of mutations found in individual ATA samples by exome sequencing.

Pat. #	Genomic location	Gene symbol	cDNA level (strand, change)	Protein level
1	chr1:236341736-236341736	*GPR137B*	+,487C->A	Leu163Ile
	chr10:1229191-1229191	*ADARB2*	-,314C->A	Gly105Val
	chr16:4411454-4411454	*CORO7-PAM16*	-,1595C->T	Arg532His
	chr17:74071300-74071300	*GALR2*	+,336C->A	Ser112Arg
	chr19:49965959-49965959	*ALDH16A1*	+,1045G->C	Ala349Pro
	chr19:55866691-55866691	*FAM71E2*	-,2746C->A	Glu916Stop
	chr4:123252489-123252489	*KIAA1109*	+,11258C->A	Ser3753Tyr
	chrX:20187551-20187551	*RPS6KA3*	-,1322C->A	Gly441Val
2	chr1:25153563-25153563	*CLIC4*	+,371A->G	Lys124Arg
	chr1:112237978-112237978	*RAP1A*	+,73C->T	Gln25Stop
	chr12:124862888-124862888	*NCOR2*	-,2062C->T	Ala688Thr
	chr16:49671856-49671856	*ZNF423*	-,856C->T	Gly286Ser
	chr17:39296648-39296648	*KRTAP4-6*	-,92C->T	Cys31Tyr
	chr17:40858152-40858152	***EZH1***	**-,1712T->C**	**Gln571Arg**
	chr2:25360264-25360264	*EFR3B*	+,1615G->A	Val539Met
	chr20:57484420-57484420	*GNAS*	+,601C->A	Arg201Ser
	chr21:37734517-37734517	*MORC3*	+,1443G->T	Met481Ile
	chr22:22869057-22869057	*ZNF280A*	-,898A->T	Cys300Ser
	chr8:104383954-104383954	*CTHRC1*	+,70C->A	Leu24Met
	chrX:27765367-27765367	*DCAF8L2*	+,355G->A	Glu119Lys
3	chr14:96811660-96811660	*ATG2B*	-,388C->T	Glu130Lys
	chr16:2013187-2013187	*RPS2*	-,338T->G	Gln113Pro
	chr4:151770700-151770700	*LRBA*	-,9_9delG	frame-shift
	chr5:149497368-149497368	*PDGFRB*	-,2950C->A	Ala984Ser
4	chr10:98823277-98823277	*SLIT1*	-,728G->T	Ser243Stop
	chr11:118252194-118252194	*UBE4A*	+,1965G->T	Glu655Asp
	chr19:3206343-3206343	*NCLN*	+,1419C->A	Ser473Arg
	chr5:72157731-72157731	*TNPO1*	+,302A->T	Asn101Ile
	chr6:42937478-42937478	*PEX6*	-,1295C->A	Ser432Ile
	chr6:70990717-70990717	*COL9A1*	-,173G->A	Pro58Leu
	chr6:170627124-170627124	*FAM120B*	+,646G->T	Gly216Cys
	chr7:47851521-47851521	*PKD1L1*	-,7475C->A	Arg2492Ile
5	chr1:202736089-202736089	*KDM5B*	-,202G->A	Pro68Ser
	chr16:4164466-4164466	*ADCY9*	-,978T->G	Glu326Asp
	chr17:40858152-40858152	***EZH1***	**-,1712T->C**	**Gln571Arg**
	chr21:43221415-43221417	*PRDM15*	-,3520_3522delCTG	Gln1194del
	chr3:49692901-49692901	*BSN*	+,5912C->T	Pro1971Leu
	chr5:90021009-90021009	*GPR98*	+,10013A->G	Asn3338Ser
	chr8:133895106-133895106	*TG*	+,937C->A	His313Asn
	chr9:115651887-115651887	*SLC46A2*	-,1075C->T	Gly359Arg

6	chr1:153430295-153430295	*S100A7*	-,293C->A	Gly98Val
	chr12:53591737-53591737	*ITGB7*	-,AG->GG	direct splice site
	chr14:81610293-81610293	*TSHR*	+,1891T->G	Phe631Val
	chr17:39458347-39458347	*KRTAP29-1*	-,757G->T	Leu253Met
	chr17:40858152-40858152	***EZH1***	**-,1712T->C**	**Gln571Arg**
	chr20:4163163-4163163	*SMOX*	+,878G->A	Arg293Gln
	chr8:37976833-37976833	*ASH2L*	+,899G->A	Arg300His
	chr8:133883736-133883736	*TG*	+,418T->G	Cys140Gly
7	chr5:180018432-180018432	*SCGB3A1*	-,31C->T	Val11Met
8	chr1:34498249-34498249	*CSMD2*	-,463G->A	Arg155Cys
	chr1:63005234-63005234	*DOCK7*	-,822T->C	Ile274Met
	chr11:14496125-14496125	*COPB1*	-,1653G->T	Phe551Le
	chr11:108709189-108709189	*DDX10*	+,1982A->G	Lys661Arg
	chr14:81610258-81610258	*TSHR*	+,1856A->G	Asp619Gly
	chr17:40858152-40858152	***EZH1***	**-,1712T->C**	**Gln571Arg**
	chr9:97088217-97088217	*NUTM2F*	-,AG->AA	direct splice site
9	chr10:101379802-101379802	*SLC25A28*	-,291C->A	Lys97Asn
	chr11:11400729-11400729	*GALNT18*	-,678G->T	Ser226Arg
	chr6:11134810-11134810	*SMIM13*	+,251A->G	Asp84Gly
10	chr17:17129614-17129614	*PLD6 FLCN*	-,272C->G	Gly91Ala
	chr6:128319908-128319908	*PTPRK*	-,311A->T	Leu104His
11	chr12:25257339-25257339	*LRMP*	+,1091C->A	Pro364His
	chr14:81609760-81609760	*TSHR*	+,1358T->C	Met453Thr
	chr15:44136131-44136131	*WDR76*	+,719G->C	Ser240Thr
	chr16:2333291-2333291	*ABCA3*	-,3931C->A	Ala1311Ser
	chr2:230642192-230642192	*TRIP12*	-,5242C->A	Asp1748Tyr
	chr6:51923291-51923291	*PKHD1*	-,1342C->T	Gly448Ser
12	chr1:116609709-116609709	*SLC22A15*	+,1624G->T	Glu542Stop
	chr1:155658111-155658119	*YY1AP1*	-,136_144 delGCGGCGGCA	Cys46_Arg48del
13	chr12:39740290-39740290	*KIF21A*	-,1690C->T	Glu564Lys
	chr14:81609760-81609760	*TSHR*	+,1358T->C	Met453Thr
	chr20:62365028-62365028	*ZGPAT*	+,808C->T	Arg270Cys
	chrX:48979013-48979013	*GPKOW*	-,290G->A	Ala97Val
14	none	-	-	-
15	chr1:247752236-247752236	*OR2G2*	+,575G->A	Cys192Tyr
	chr10:89711927-89711928	*PTEN*	+,545_546insA	frame-shift
	chr13:114514818-114514818	*TMEM255B*	+,923C->T	Pro308Leu
	chr19:2227734-2227734	*DOT1L*	+,AG->TG	direct splice site
	chr19:37210785-37210785	*ZNF567*	+,1159C->G	His387Asp
	chr7:106509733-106509733	*PIK3CG*	+,1727G->A	Trp576Stop
16	chr10:101455722-101455722	*ENTPD7*	+,853G->A	Ala285Thr
	chr11:56237195-56237195	*OR5M3*	-,779C->T	Arg260His
	chr12:88566483-88566483	*TMTC3*	+,1160T->C	Ile387Thr

	chr14:81609760-81609760	*TSHR*	+,1358T->C	Met453Thr
17	chr6:17626091-17626091	*NUP153*	-,3942A->T	Asn1314Lys
	chr6:106727653-106727653	*ATG5*	-,361T->C	Ile121Val
	chr7:73097974-73097974	*WBSCR22*	+,19C->T	Arg7Cys
	chr9:35062228-35062228	*VCP*	-,931G->A	Pro311Ser
18	chr1:19181005-19181005	*TAS1R2*	-,959C->A	Gly320Val
	chr10:50533915-50533915	*C10orf71*	+,3325C->T	Arg1109Trp
	chr11:85435939-85435939	*SYTL2*	-,1561_1561delC	frame-shift
	chr2:179718350-179718350	*CCDC141*	-,1499C->T	Cys500Tyr
	chr20:43945531-43945531	*RBPJL*	+,1486G->T	Asp496Tyr
	chr20:48130848-48130848	*PTGIS*	-,940C->T	Glu314Lys
	chr3:32932671-32932671	*TRIM71*	+,1975G->A	Val659Met
19	none	-	-	-

Supplemental Table 2. Canonical pathway analysis of candidate mutated genes identified by exome sequencing.

Gene Set Name [# Genes (K)]	Description	Genes in Overlap	p-value	FDR q-value
PID_PDGFRB_PATHWAY [129]	PDGFR-beta signaling pathway	*PIK3CG PTEN RAP1A PDGFRB RPS6KA*	3.48 e^{-6}	4.63 e^{-3}
KEGG_FOCAL_ADHESION [201]	Focal adhesion	*PIK3CG PTEN RAP1A PDGFRB ITGB7*	2.98 e^{-5}	1.31 e^{-2}
REACTOME_SIGNALING_BY_GPCR [920]	Genes involved in Signaling by GPCR	*PIK3CG RPS6KAA DCY9 GNAS TSHR GALR2 OR5M3 OR2G2 TAS1R2*	3.58 e^{-5}	1.31 e^{-2}
BIOCARTA_MET_PATHWAY [37]	Signaling of Hepatocyte Growth Factor Receptor	*PIK3CG PTEN RAP1A*	3.92 e^{-5}	1.31 e^{-2}
REACTOME_SIGNALING_BY_PDGF [122]	Genes involved in Signaling by PDGF	*PTEN PDGFRB ADCY9 COL9A1*	6.72 e^{-5}	1.79 e^{-2}
PID_PI3KCI_PATHWAY [49]	Class I PI3K signaling events	*PIK3CG PTEN RAP1A*	9.17 e^{-5}	2.0 e^{-2}
REACTOME_NGF_SIGNALLING_VIA_TRKA_FROM_THE_PLASMA_MEMBRANE [137]	Genes involved in NGF signaling via TRKA from the plasma membrane	*PTEN RAP1A RPS6KAA DCY9*	1.05 e^{-4}	2.0 e^{-2}
KEGG_GLIOMA [65]	Glioma	*PIK3CG PTEN PDGFRB*	2.13 e^{-4}	3.06 e^{-2}
PID_ERA_GENOMIC_PATHWAY [65]	Validated nuclear estrogen receptor alpha network	*ABCA3 NCOR2 PRDM15*	2.13 e^{-4}	3.06 e^{-2}
REACTOME_IMMUNE_SYSTEM [933]	Genes involved in Immune System	*PTEN RAP1A PDGFRB ITGB7 NUP153 TRIP12*	2.44 e^{-4}	3.06 e^{-2}

		UBE4A *ATG5*		
KEGG_RENAL_CELL_CARCINOMA [70]	Renal cell carcinoma	*PIK3CG* *RAP1A* *FLCN*	$2.65\ e^{-4}$	$3.06\ e^{-2}$
KEGG_MELANOMA [71]	Melanoma	*PIK3CG* *PTEN* *PDGFRB*	$2.77\ e^{-4}$	$3.06\ e^{-2}$

Supplemental Table 3. Clinical data and genetic results of the ATA cases included in exome sequencing

Pat. #	sex	age at surgery (years)	tumor size (mm)	TSH (mU/L)	FT4 (pmol/L)	FT3 (pmol/L)	AbTg/ AbTPO	*TSHR*	*GNAS*	*EZH1*
1	M	56	31	<0.05	20.1	N/A	N/A	WT	WT	WT
2	F	74	38	0.01	28.4	10.5	neg	WT	R201S	**Q571R**
3	F	50	25	0.03	15.31	6.13	neg	WT	WT	WT
4	M	36	35	0.54	17.1	7.2	neg	WT	WT	WT
5	F	73	22	<0.01	20.2	N/A	neg	WT	WT	**Q571R**
6	M	56	15	0.44	15.55	6.53	neg	F631V	WT	**Q571R**
7	F	52	43	0.01	21.5	8.72	neg	WT	WT	WT
8	F	63	35	<0.01	20.0	7.53	N/A	D619G	WT	**Q571R**
9	F	66	15	0.1	101 nmol/L (TT4)	1.59 nmol/L (TT3)	N/A	WT	WT	WT
10	M	68	23	0.72	12.0	4.5	neg	WT	WT	WT
11	F	53	29	0.04	15.7	5.68	N/A	M453T	WT	WT
12	F	75	17	<0.005	17.63	5.54	N/A	WT	WT	WT
13	F	51	44	0.093	21.49	8.33	N/A	M453T	WT	WT
14	F	52	54	1.36	15.83	5.21	32.18	WT	WT	WT
15	F	49	40	0.657	14.29	5.31	8.23	WT	WT	WT
16	F	55	31	0.08	21.9	5.7	N/A	M453T	WT	WT
17	F	62	32	0.24	–	–	neg	WT	WT	WT
18	F	57	37	0.1	–	–	neg	WT	WT	WT
19	F	73	43	0.2	–	–	neg	WT	WT	WT

Normal ranges: TSH = 0.27–4.2 mU/L; FT4 = 10–23 pmol/L; FT3 = 3.5–9.0 pmol/L; WT = wild type.

Supplemental Table 4. Clinical, hormonal and genetic data of 94 patients with autonomous thyroid adenomas. Patients with normal TSH were receiving anti-thyroid drugs at the moment of surgery.

	Sex/Age at Surgery (years)	Tumor Size (mm)	TSH (mU/L)	FT4 (pmol/L)	FT3 (pmol/L)	AbTG/ AbTPO	*TSHR*	*GNAS*	*EZH1*
1	M/62	30	0.686	16.60	5.15	neg	WT	Q227H	WT
2	F/67	25	0.495	13.38	5.19	neg	H271N	rs1004902	WT
3	F/44	50	<0.005	13.00	4.50	neg	M453T	WT	WT
4	F/50	31	<0.005	14.03	4.87	neg	WT	WT	WT
5	F/61	25	0.254	N/A	3.90	neg	T632A	WT	Q571R
6	F/66	29	<0.006	7.85	3.61	neg	T632I	WT	WT
7	F/46	39	5.02	11.33	5.30	neg	WT	WT	WT
8	F/56	46	0.08	14.93	3.16	neg	I486M	WT	WT
9	F/63	20	0.01	13.77	5.15	neg	A428I	rs1004902	Q571R
10	F/65	57	<0.005	N/A	N/A	neg	WT	WT	Q571R
11	M/66	60	<0.005	17.89	5.67	neg	L629F	WT	WT
12	M/64	15	0.011	N/A	N/A	neg	WT	WT	WT
13	F/21	48	0.07	7.98	5.73	neg	F631I	WT	WT
14	F/70	36	0.04	23.68	8.26	neg	I486M	WT	WT
15	F/62	24	<0.005	20.59	4.21	neg	WT	WT	Q571R
16	F/53	29	0.04	15.70	5.68	neg	M453T	WT	WT
17	F/37	70	0.25	10.04	6.91	neg	L430L / F631L	WT	Q571R
18	F/75	17	<0.005	17.63	5.54	neg	WT	WT	WT
19	M/48	43	0.03	12.23	5.99	neg	L430L	WT	WT
20	F/63	38	0.21	11.71	4.62	neg	I486M	I185I	Q571R
21	F/36	18	0.09	8.11	5.15	neg	WT	rs1004902	WT
22	F/30	33	0.867	9.78	4.45	neg	D633H	WT	WT
23	F/45	37	0.102	23.17	6.17	neg	D633E	WT	Q571R
24	F/64	30	1.13	19.69	5.02	neg	WT	rs1004902	WT
25	M/62	37	1.81	20.85	6.10	neg	WT	rs1004902	WT
26	F/28	45	0.862	13.64	5.70	neg	WT	WT	WT
27	F/52	44	0.017	16.86	5.79	neg	WT	WT	WT
28	M/57	22	0.754	12.10	5.11	neg	L629F	WT	Q571R
29	F/57	39	0.012	17.50	5.93	neg	A623C	WT	WT
30	F/51	44	0.093	21.49	8.33	neg	M453T	WT	WT
31	F/49	41	0.025	11.58	4.99	neg	S281N	WT	WT
32	F/60	37	1.82	16.34	9.57	neg	WT	WT	Q571R
33	F/52	54	1.36	15.83	5.21	neg	WT	WT	WT
34	M/58	39	0.843	12.10	5.04	neg	A623V	WT	Q571R
35	M/56	26	2.3	N/A	N/A	neg	WT	WT	WT
36	F/65	41	0.005	28.56	11.62	N/A	D633Y	WT	WT
37	F/37	30	<0.005	29.08	7.79	N/A	D633Y	WT	WT
38	F/58	45	0.005	57.32	16.08	N/A	WT	WT	WT
39	M/62	37	<0.005	38.75	14.01	N/A	T632I	WT	WT
40	M/62	8	<0.005	38.75	14.01	N/A	A623V	WT	Q571R
41	F/43	33	<0.005	29.5	10	N/A	M453T	WT	WT
42	F/54	10	1.84	17.64	5.13	N/A	WT	WT	WT
43	F/54	25	1.84	17.64	5.13	N/A	N372T	WT	WT

44	M/58	20	0.089	13.9	6.12	N/A	WT	WT	WT
45	M/58	35	0.089	13.9	6.12	N/A	WT	WT	WT
46	M/72	45	<0.005	23.92	6.37	N/A	WT	WT	Q571R
47	F/54	20	<0.005	38.71	9.88	N/A	D619G	WT	WT
48	F/54	12	<0.005	38.71	9.88	N/A	D619G	WT	WT
49	F/71	39	0.005	35.26	10.08	N/A	D619G	WT	WT
50	F/45	42	<0.005	52.25	19.52	N/A	M453T	WT	Q571R
51	F/41	24	0.208	4.92	5.3	N/A	V656F	WT	Q571R
52	F/52	33	0.053	58.62	27.06	N/A	L512Q	WT	Q571R
53	F/31	45	<0.005	>100	33.0	N/A	T632I	WT	WT
54	F/31	61	<0.005	>100	33.0	N/A	L512Q	WT	WT
55	F/45	61	0.005	86.23	29.07	N/A	M453T	WT	WT
56	F/45	42	0.005	86.23	29.07	N/A	T632I	WT	WT
57	F/50	75	<0.005	45.76	47.61	N/A	T632A	WT	Q571R
58	F/54	25	0.046	18.7	6.06	N/A	WT	WT	WT
59	F/54	35	0.046	18.7	6.06	N/A	M453T	WT	WT
60	F/48	35	0.012	38.3	14.4	N/A	M453T	WT	WT
61	F/48	10	0.012	38.3	14.4	N/A	L629F	WT	WT
62	F/38	25	<0.002	16.09	5.09	N/A	WT	WT	WT
63	F/38	34	<0.002	16.09	5.09	N/A	486F	WT	WT
64	M/66	42	0.005	24.03	10.31	N/A	I486N	WT	Q571R
65	F/72	41	0.015	>100	41.8	N/A	T632I	WT	Q571R
66	F/72	23	0.015	>100	41.8	N/A	L629F	WT	Q571R
67	F/43	43	0.9	14.02	5.48	N/A	D633Y	WT	WT
68	F/37	37	0.005	18.0	6.15	N/A	D619G	WT	Q571R
69	M/43	54	0.005	31.3	10.13	N/A	F631L	WT	Q571R
70	F/48	44	0.008	26.1	10.13	N/A	T632I	WT	WT
71	M/64	45	0.03	18.06	10.78	N/A	T632I	WT	Q571R
72	M/57	43	0.03	23.22	10.78	N/A	N372T	WT	WT
73	F/54	40	0.021	27.8	8.71	N/A	T632A	WT	WT
74	F/53	34	0.008	26.7	6.72	N/A	S505N	WT	WT
75	F/43	35	0.9	17.9	5.87	N/A	L629F	WT	Q571R
76	F/60	31	0.035	27.8	9.27	N/A	A623V	WT	Q571R
77	F/47	12	0.046	25.67	11.59	N/A	WT	WT	WT
78	F/47	12	0.046	25.67	11.59	N/A	WT	WT	WT
79	F/60	51	0.026	23.1	8.75	N/A	P639S	WT	WT
80	F/72	24	0.081	36.7	11.0	N/A	WT	WT	WT
81	F/72	20	0.081	36.7	11.0	N/A	WT	WT	WT
82	F/48	54	<0.005	31.31	12.7	N/A	M453T	WT	Q571R
83	F/35	26	0.3	21.6	6.8	N/A	S281N	WT	WT
84	F/26	19	0.005	36	5.4	N/A	I568T	WT	WT
85	M/42	53	0.2	13.9	6.69	N/A	D633H	WT	WT
86	F/59	28	0.1	27.4	4.99	N/A	WT	WT	WT
87	F/56	40	0.1	25.6	7.04	N/A	I630L	WT	WT
88	F/56	20	0.1	25.6	7.04	N/A	A627V	WT	WT
89	F/44	10	0.005	33.34	13.16	N/A	A428V	WT	WT
90	F/44	34	0.005	33.34	13.16	N/A	WT	WT	WT
91	F/65	32	0.3	14.05	5.08	N/A	WT	WT	WT
92	F/35	8	0.028	39.06	8.71	N/A	WT	WT	WT
93	F/35	31	0.028	39.06	8.71	N/A	L512R	WT	WT

94	F/24	41	0.03	29.03	8.08	N/A	F632L	WT	WT

Normal ranges: TSH = 0.27–4.2 mU/l; FT4 = 10–23 pmol/l; FT3 = 3.5–9.0 pmol/l; WT = wild type. No correlation was found between mutational status and clinical parameters.

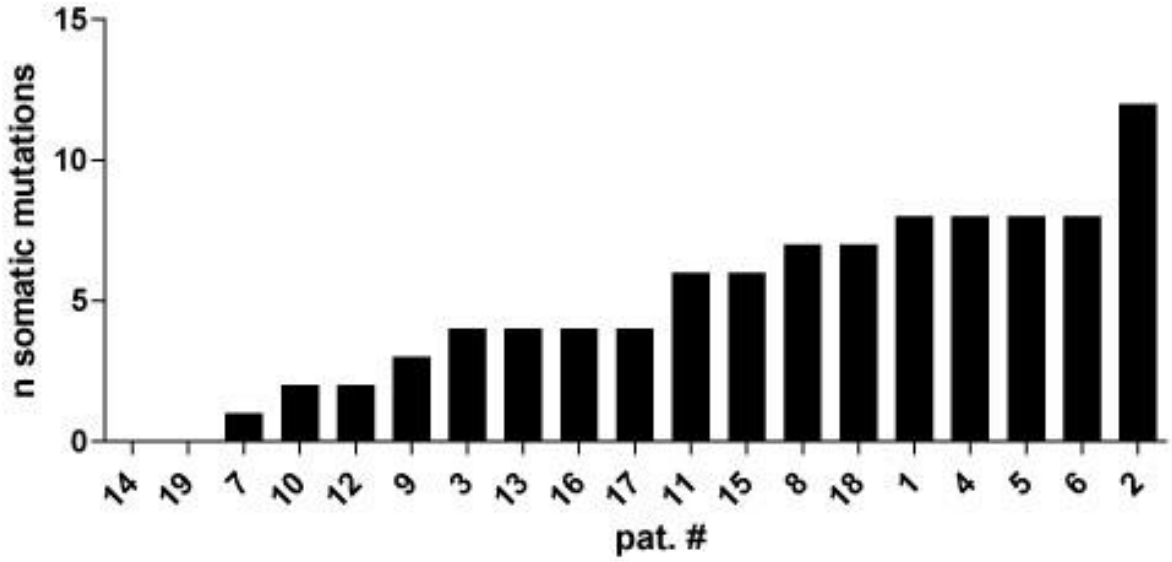

Supplemental Figure 1. Number of mutations found in each ATA sample by exome sequencing.

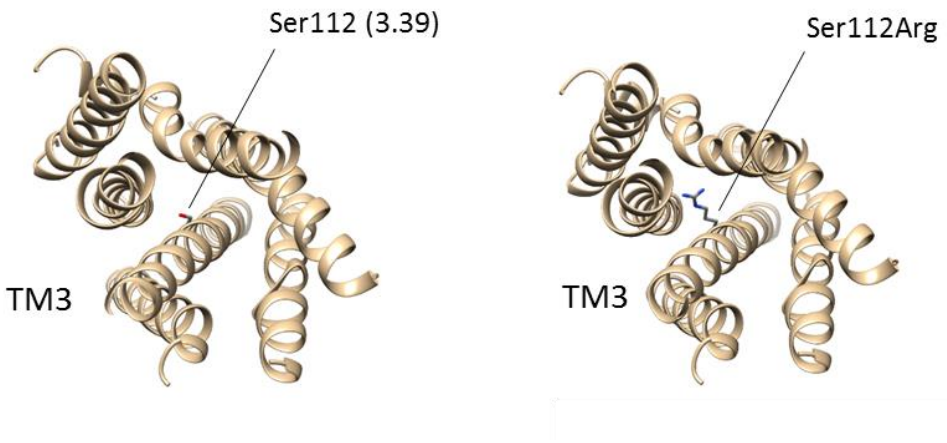

Supplemental Figure 2. Location of the Ser112 residue (left) and Ser112Arg substitution (right) in the 3TM domain of GALR2. Shown is a homology model of GALR2, based on the GPCR-Sequence-Structure-Feature-Extractor (SSFE) database (available at http://www.ssfa-7tmr.de/ssfe/index.php). The receptors are viewed from the top (i.e. from the extracellular side).

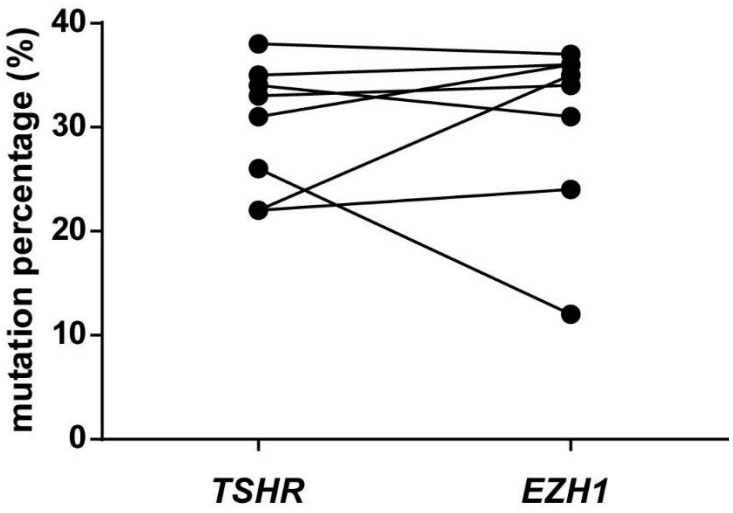

Supplemental Figure 3. Allelic percentage of *TSHR* and *EZH1* mutation in ATAs. For 8 ATAs harboring both a *TSHR* and an *EZH1* mutation the allelic percentages of the *TSHR* and of the *EZH1* mutation were compared by pyrosequencing. In 6 out of the 8 ATAs the allelic percentages was nearly identical (median 34% vs. 35%, respectively), suggesting a possible clonal origin of the cells harboring both mutations.

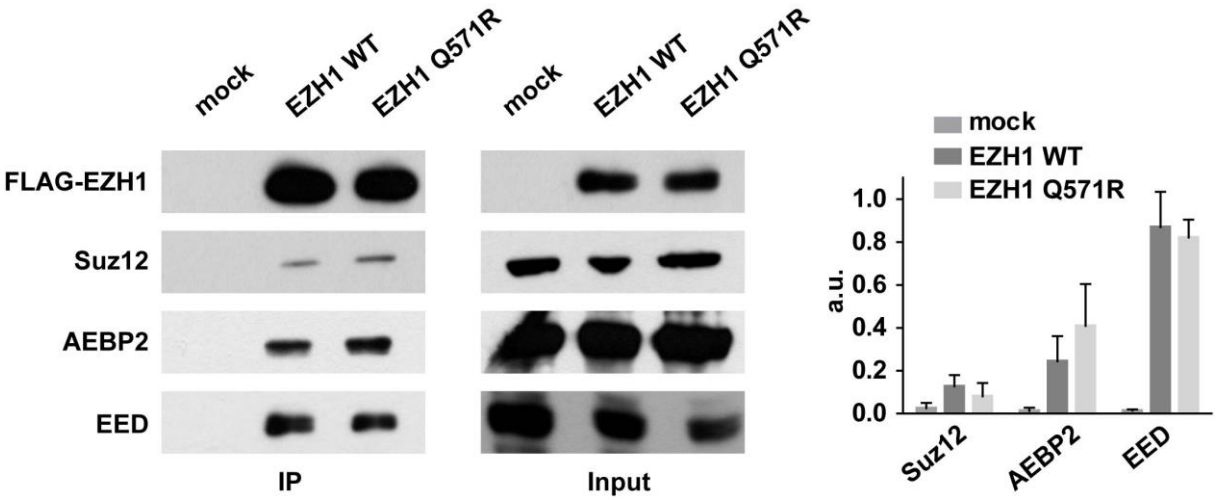

Supplemental Figure 4. Co-immunoprecipation between wild-type or mutant EZH1 and components of the PRC2 complex. HEK293 cells were transiently transfected with FLAG-tagged EZH1 constructs (WT or Q571R mutant) and cell lysates were immunoprecipitated with an anti-FLAG antibody. Suz12, AEBP2 and EED were detected by western blot analysis with specific antibodies. Left, representative experiment. Right, densitometry quantification of the results of three independent experiments. Shown are the intensity levels (mean ± SEM) of the bands in the immunoprecipitated samples (IP), expressed in arbitrary units (a.u.).

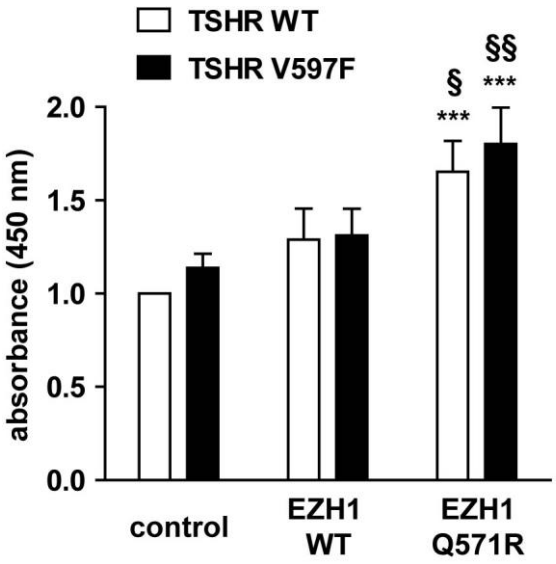

Supplemental Figure 5. Effect of transient transfection of the EZH1 mutant on the proliferation of FRT cells stably expressing the wild-type (WT) receptor or a constitutively active TSHR mutant (V597F). Cell viability was measured 72 h after the transfection with the MTT assay as the absorbance at 450 nm. The cells were grown in the absence of TSH. Data in **B** (mean ± SEM) are from 4 independent experiments per condition. Differences were statistically significant by two-way ANOVA followed by Tukey´s multiple comparison test. P values are given compared to the corresponding condition in the control or EZH1 WT group. ***, $P < 0.001$ vs control. §, $P<0.05$ vs. EZH1 WT. §§, $P<0.01$ vs. EZH1 WT.

References

1. Sancak S, Jaeschke H, Eren F, Tarcin O, Guellueoglu B, Sen LS, Sever Z, Gozu HI, Bircan R, Akalin S, et al. High prevalence of TSHR/Gsalpha mutation-negative clonal hot thyroid nodules (HNs) in a Turkish cohort. *Hormone and metabolic research.* 2011;43(8):562-8.
2. Gözü HI, Bircan R, Krohn K, Muller S, Vural S, Gezen C, Sargin H, Yavuzer D, Sargin M, Cirakoglu B, et al. Similar prevalence of somatic TSH receptor and Gsalpha mutations in toxic thyroid nodules in geographical regions with different iodine supply in Turkey. *Eur J Endocrinol.* 2006;155(4):535-45.
3. Eszlinger M, Niedziela M, Typlt E, Jaeschke H, Huth S, Schaarschmidt J, Aigner T, Trejster E, Krohn K, Bosenberg E, et al. Somatic mutations in 33 benign and malignant hot thyroid nodules in children and adolescents. *Mol Cell Endocrinol.* 2014;393(1-2):39-45.
4. Lueblinghoff J, Mueller S, Sontheimer J, and Paschke R. Lack of consistent association of thyrotropin receptor mutations in vitro activity with the clinical course of patients with sporadic non-autoimmune hyperthyroidism. *J Endocrinol Invest.* 2010;33(4):228-33.
5. Lueblinghoff J, Eszlinger M, Jaeschke H, Mueller S, Bircan R, Gozu H, Sancak S, Akalin S, and Paschke R. Shared sporadic and somatic thyrotropin receptor mutations display more active in vitro activities than familial thyrotropin receptor mutations. *Thyroid.* 2011;21(3):221-9.
6. Adzhubei IA, Schmidt S, Peshkin L, Ramensky VE, Gerasimova A, Bork P, Kondrashov AS, Sunyaev SR. A method and server for predicting damaging missense mutations. *Nat Methods* 2010;7(4):248-249.
7. Exome Aggregation Consortium, Monkol Lek, Konrad Karczewski, Eric Minikel, Kaitlin Samocha, Eric Banks, Timothy Fennell, Anne O'Donnell-Luria, James Ware, Andrew Hill, Beryl Cummings, Taru Tukiainen, Daniel Birnbaum, Jack Kosmicki, Laramie Duncan, Karol Estrada, Fengmei Zhao, James Zou, Emma Pierce-Hoffman, David Cooper, Mark DePristo, Ron Do, Jason Flannick, Menachem Fromer, Laura Gauthier, Jackie Goldstein, Namrata Gupta,

Daniel Howrigan, Adam Kiezun, Mitja Kurki, Ami Levy Moonshine, Pradeep Natarajan, Lorena Orozco, Gina Peloso, Ryan Poplin, Manuel Rivas, Valentin Ruano-Rubio, Douglas Ruderfer, Khalid Shakir, Peter Stenson, Christine Stevens, Brett Thomas, Grace Tiao, Maria Tusie-Luna, Ben Weisburd, Hong-Hee Won, Dongmei Yu, David Altshuler, Diego Ardissino, Michael Boehnke, John Danesh, Elosua Roberto, Jose Florez, Stacey Gabriel, Gad Getz, Christina Hultman, Sekar Kathiresan, Markku Laakso, Steven McCarroll, Mark McCarthy, Dermot McGovern, Ruth McPherson, Benjamin Neale, Aarno Palotie, Shaun Purcell, Danish Saleheen, Jeremiah Scharf, Pamela Sklar, Sullivan Patrick, Jaakko Tuomilehto, Hugh Watkins, James Wilson, Mark Daly, Daniel MacArthur. Analysis of protein-coding genetic variation in 60,706 humans. Preprint at http://www.biorxiv.org/content/early/2015/10/30/030338

8. Eden E, Navon R, Steinfeld I, Lipson D, and Yakhini Z. GOrilla: a tool for discovery and visualization of enriched GO terms in ranked gene lists. *BMC Bioinformatics.* 2009;10:48.

9. Subramanian A, Tamayo P, Mootha VK, Mukherjee S, Ebert BL, Gillette MA, Paulovich A, Pomeroy SL, Golub TR, Lander ES, et al. Gene set enrichment analysis: a knowledge-based approach for interpreting genome-wide expression profiles. *Proc Natl Acad Sci U S A.* 2005;102(43):15545-50.

10. Ciferri C, Lander GC, Maiolica A, Herzog F, Aebersold R, and Nogales E. Molecular architecture of human polycomb repressive complex 2. *eLife.* 2012;1:e00005.

11. Pettersen EF, Goddard TD, Huang CC, Couch GS, Greenblatt DM, Meng EC, and Ferrin TE. UCSF Chimera–a visualization system for exploratory research and analysis. *Journal of computational chemistry.* 2004;25(13):1605-12.

12. Calebiro D, de Filippis T, Lucchi S, Martinez F, Porazzi P, Trivellato R, Locati M, Beck-Peccoz P, and Persani L. Selective modulation of protein kinase A I and II reveals distinct roles in thyroid cell gene expression and growth. *Mol Endocrinol.* 2006;20(12):3196-211.

13. Calebiro D, Hannawacker A, Lyga S, Bathon K, Zabel U, Ronchi C, Beuschlein F, Reincke M, Lorenz K, Allolio B, et al. PKA catalytic subunit mutations in adrenocortical Cushing's adenoma impair association with the regulatory subunit. *Nature communications.* 2014;5:5680.

14. Nitsch L, Tramontano D, Ambesi-Impiombato FS, Quarto N, and Bonatti S. Morphological and functional polarity of an epithelial thyroid cell line. *Eur J Cell Biol.* 1985;38(1):57-66.

15. Shechter D, Dormann HL, Allis CD, and Hake SB. Extraction, purification and analysis of histones. *Nat Protoc.* 2007;2(6):1445-57.

16. Yap DB, Chu J, Berg T, Schapira M, Cheng SW, Moradian A, Morin RD, Mungall AJ, Meissner B, Boyle M, Marquez VE, Marra MA, Gascoyne RD, Humphries RK, Arrowsmith CH, Morin GB, Aparicio SA. Somatic mutations at EZH2 Y641 act dominantly through a mechanism of selectively altered PRC2 catalytic activity, to increase H3K27 trimethylation. *Blood*. 2011;117(8):2451-9.

17. Liu W, Chun E, Thompson AA, Chubukov P, Xu F, Katritch V, Han GW, Roth CB, Heitman LH, IJzerman AP, Cherezov V, Stevens RC. Structural basis for allosteric regulation of GPCRs by sodium ions. *Science.* 2012;337(6091):232-6.